photonics

MDPI

Article

Microwave Frequency Dissemination over a 212 km Cascaded Urban Fiber Link with Stability at the 10^{-18} Level

Honglei Quan [1,2,3], Wenxiang Xue [1,2], Wenyu Zhao [1,2,3,*], Yan Xing [1,2], Haifeng Jiang [1,2,3,4], Wenge Guo [1,2,5] and Shougang Zhang [1,2,3]

1 National Time Service Center, Chinese Academy of Sciences, 3 Shuyuandong Road, Xi'an 710600, China; quanhonglei17@mails.ucas.ac.cn (H.Q.); xuewenxiang@ntsc.ac.cn (W.X.); xingyan@ntsc.ac.cn (Y.X.); hjiang1@ustc.edu.cn (H.J.); wguo@xsyu.edu.cn (W.G.); szhang@ntsc.ac.cn (S.Z.)
2 Key Laboratory of Time and Frequency Standards, Chinese Academy of Sciences, 3 Shuyuandong Road, Xi'an 710600, China
3 School of Astronomy and Space Science, University of Chinese Academy of Sciences, 19 Yuquan Road, Beijing 100049, China
4 School of Physics Sciences, University of Science and Technology of China, Hefei 230026, China
5 School of Science, Xi'an Shiyou University, 18 East Section of Electronic Second Road, Xi'an 710065, China
* Correspondence: zhaowy@ntsc.ac.cn

Abstract: To synchronize standard frequency signals between long-distance laboratories, we carried out a frequency dissemination experiment over a 212 km cascaded urban fiber link. This cascaded link was composed of two 106 km fiber links, in which the fiber noise was compensated by two microwave frequency dissemination systems. The two adjacent frequency dissemination systems used different frequency transmitted signals, preventing the influence of signal crosstalk between the received signal of the previous stage and the transmitted signal of the second stage caused by microwave signal leakage. The frequency dissemination over the cascaded link showed a dissemination fractional frequency instability of 6.2×10^{-15} at 1 s and 6.4×10^{-18} at 40,000 s, which is better than the transfer stability over the same 212 km single-stage link.

Keywords: fiber; microwave; frequency; dissemination; cascaded link

check for updates

Citation: Quan, H.; Xue, W.; Zhao, W.; Xing, Y.; Jiang, H.; Guo, W.; Zhang, S. Microwave Frequency Dissemination over a 212 km Cascaded Urban Fiber Link with Stability at the 10^{-18} Level. *Photonics* **2022**, *9*, 399. https://doi.org/10.3390/photonics9060399

Received: 25 April 2022
Accepted: 31 May 2022
Published: 6 June 2022

Publisher's Note: MDPI stays neutral with regard to jurisdictional claims in published maps and institutional affiliations.

Copyright: © 2022 by the authors. Licensee MDPI, Basel, Switzerland. This article is an open access article distributed under the terms and conditions of the Creative Commons Attribution (CC BY) license (https://creativecommons.org/licenses/by/4.0/).

1. Introduction

The dissemination of ultra-stable standard frequency signals is required for many applications such as radio astronomy observations [1–4], remote atomic clock signal comparison [5], geodetic measurements [6,7], and fundamental physics research [8–10]. Traditional satellite-based frequency dissemination was limited to the fractional frequency stability of 10^{-16} after one-day averaging time due to the resolution limitation of the microwave carrier [11–14]. Benefiting from low attenuation, high reliability, continuous availability, and wide distributions of communication fiber links, fiber-based optical frequency or microwave frequency dissemination has been demonstrated with high stability [15–21]. For microwave frequency dissemination, optical phase compensation and microwave phase compensation are the two main link noise compensation schemes. In 2009, based on optical phase compensation, a 9.1 GHz signal was transferred through 86 km urban fiber link, exhibiting stabilities of 1×10^{-15} at 1s and below 10^{-18} after one day of integration time [19]. In 2012, based on microwave phase compensation, an atomic clock signal was synchronized across 80 km urban fiber link, exhibiting stabilities of 7×10^{-15} at 1 s and 4.5×10^{-19} at 10^5 s [22]. The current challenge is to extend the distance of microwave frequency dissemination over urban fiber links. For longer transfer distance, the signal-to-noise ratio (SNR) of the microwave signal detected by the photodetector degrades seriously due to the signal attenuation and chromatic dispersion of the fiber link. In addition, the phase noise suppression bandwidth also decreases. These factors decrease the stability of fiber-based frequency dissemination.

Microwave frequency dissemination through a cascaded link can be a better choice to realize long-distance high-resolution dissemination. In 2016, based on optical phase compensation, a 10 MHz atomic maser signal was transferred over 230 km cascaded fiber links with the stability of 3.1×10^{-14} at 1s and 6.3×10^{-18} at 10^4 s [23]. In 2015, based on microwave phase compensation, a 9.1 GHz signal was synchronized through 145 km cascaded fiber link, with a relative frequency stability of 1.3×10^{-14} at 1s and 4.1×10^{-17} at 10^4 s [24]. For optical phase compensation, the compensation actuator usually consists of a piezoelectric fiber stretcher and temperature-controlled optical delay line, which is complex and bulky. The piezoelectric fiber stretcher also induces polarization mode dispersion noise. For microwave phase compensation, the compensation actuator is a voltage-controlled oscillator, which is more suitable for engineering applications. So far, for the microwave phase compensation scheme, the influence of signal crosstalk caused by microwave leakage on frequency dissemination over cascaded links has not attracted attention. If two adjacent stages use dissemination signals with the same frequency, the phase varying transmitted signal will crosstalk with the received signal of the previous stage due to microwave leakage, which decreases dissemination stability.

This study is arranged as follows: in Section 2, we describe the principle of the microwave frequency dissemination system. In Section 3, we report the experiment of microwave frequency dissemination over cascaded 212 km fiber links in which two adjacent frequency dissemination systems used different frequency transmission signals to prevent the influence of signal crosstalk. In Section 4, the experiment results are presented and discussed.

2. Theory

The schematic diagram of the microwave frequency dissemination system is shown in Figure 1. The reference signal of the dissemination system can be expressed as $V_r = \sin(\omega_r t + \varphi_r)$. A phase-locked dielectric oscillator (PDRO) referenced to a 100 MHz oven-controlled crystal oscillator (OCXO) generated transmitted signal $V_0 = \sin(\omega_0 t + \varphi_0)$. The transmitted signal V_0 modulated the intensity of a light beam, through a Mach–Zehnder Modulator (MZM). Then, the V_0 was transmitted to the remote over the fiber link. At the remote, the modulated signal was detected with a photodiode, expressed as $V_1 = \sin(\omega_0 t + \varphi_0 + \varphi_p)$, φ_p represents the phase perturbations of transmitted signal accumulated over the fiber link. A portion of V_1 was divided by N, to prevent the influence of parasitic reflection. Next, the resultant signal was transmitted back to local. The return signal was detected by another photodiode and can be expressed as: $V_2 = \sin\left(\frac{\omega_0 t + \varphi_0 + 2\varphi_p}{N}\right)$. The demodulated signal V_2 was input into the phase-noise detection module. In the phase-noise detection module, the returned signal V_2 mixed with V_r, producing V_b. The transmitted signal V_0 mixed with V_r and the mixed signal was divided with a 4-prescaler producing V_a. V_a mixed with V_b, providing error signal V_e.

$$V_e = \sin\left(\frac{((N+1)\omega_r - 2\omega_0)t + (N+1)\varphi_r - 2\varphi_0 - 2\varphi_p}{N}\right) \quad (1)$$

As we can see from Equation (1), this error signal contains the phase noise accumulated along the link and the phase difference between the VCO and the reference signal. So, when ω_0 and ω_r satisfy the relation of $\omega_0 = \frac{N+1}{2}\omega_r$, the phase-lock loop will control the phase of transmitted signal to maintain it at $\varphi_0 = \frac{N+1}{2}\varphi_r - \varphi_p$. Hence, the received signal at the remote can be expressed as $V_1 = \sin\left(\frac{N+1}{2}\omega_r t + \frac{N+1}{2}\varphi_r\right)$, which is referenced to the reference signal V_r at the local site.

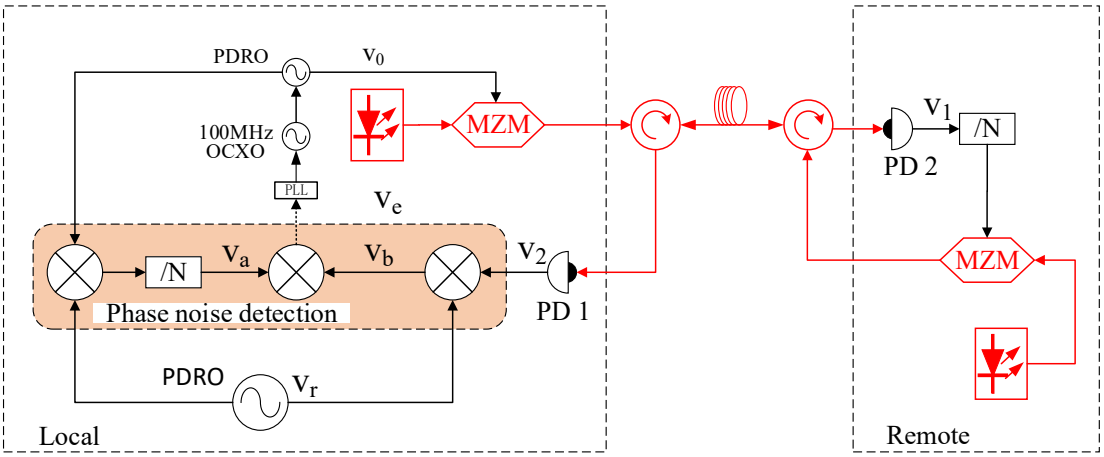

Figure 1. Scheme of the microwave frequency dissemination system; PDRO: phase-lock dielectric resonance oscillator; OCXO: oven-controlled crystal oscillator; MZM: Mach–Zehnder modulator; PD: photodetector.

In addition, the transfer stability can be computed directly from the phase noise $S(f)$ as follows [25]:

$$\sigma(\tau) = \sqrt{2\int_0^\infty (f/v_0)^2 S(f) sin^4(\pi\tau f)/(\pi\tau f)^2 df} \quad (2)$$

where $S(f)$ is the phase noise of the receive signal referred to the reference signal of local site, which is determined by the system noise floor of the dissemination system $S_{floor}(f)$ and residual phase noise introduced by the fiber link $S_{residual}(f)$. v_0 is the frequency of the measured signal.

However, longer distance the microwave frequency dissemination over an urban communication fiber link is not straightforward. The signal-to-noise ratio (SNR) of the microwave signal detected by the photodetector degrades seriously due to the signal attenuation and chromatic dispersion of the fiber link. The phase noise suppression bandwidth also decreases. Consequently, for longer distances, the microwave frequency dissemination over cascaded link is an effective means, with which the long-distance communication fiber is divided into several stages.

3. Dissemination over a 212 km Urban Cascaded Fiber Link

We performed the microwave frequency dissemination experiment on two parallel 106 km-long round-trip Lintong site–Changan site–Lintong site urban fiber links, as shown in Figure 2. The loss over each round-trip 106 km urban fiber link was about 33 dB, measured by an optical time domain reflectometer (OTDR), greater than the nominal loss (106 km $\times$ 0.2 dB/km) due to the presence of many fiber connectors of urban communication fibers. Four ends were collocated at the Lintong site, which we labelled local 1, remote 1, local 2, and remote 2.

We established two microwave frequency dissemination systems: one with 10 GHz transmitted signal and the other with 9 GHz transmitted signal. The frequency division factor N was selected as 4. According to the principle of the microwave frequency dissemination system, the reference signals of the 10 GHz and 9 GHz dissemination systems were 4 GHz and 3.6 GHz, respectively. We connected two dissemination systems in series, as shown in Figure 3. All local and remote sites were installed in the Lintong site of NTSC. A 100 MHz frequency signal from a Passive Hydrogen maser (H-maser) was used as reference signal for the whole cascaded dissemination system. At local 1, the 100 MHz reference signal was converted to 4 GHz signal, using a 4 GHz phase-locked dielectric oscillator (PDRO). Then the resultant 4 GHz signal was input into the 10 GHz dissemination system.

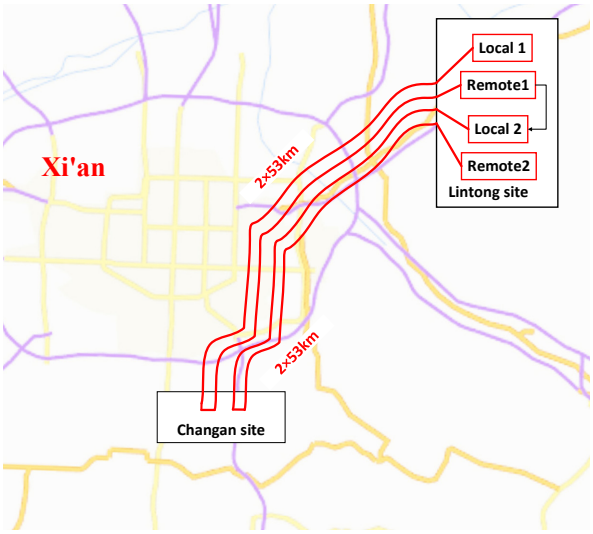

Figure 2. Diagram of the urban fiber links.

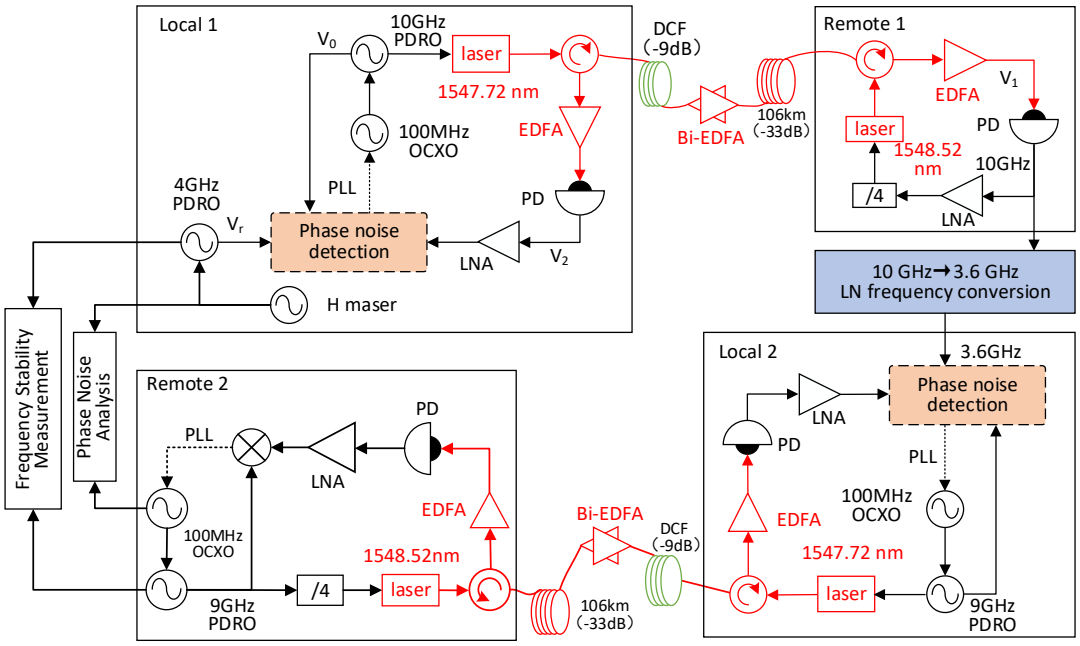

Figure 3. Scheme of the cascaded microwave frequency dissemination system; LNA: low-noise amplifier; Bi-EDFA: bidirectional Er-doped fiber optical amplifier; EDFA: unidirectional Er-doped fiber optical amplifier; DCF: dispersion compensation fiber; PD: photodetector; PDRO: phase-lock dielectric resonance oscillator; OCXO: oven-controlled crystal oscillator; MZM: Mach–Zehnder modulator; PD: photodetector.

In a cascaded dissemination system, if two adjacent dissemination systems use transmitted signals with same frequency, the phase of received signal of remote 1 crosstalk with the pre-compensation transmitted signal of local 2. Moreover, the phase of the transmitted signal of local 2 varies, which decreases the dissemination stability [26]. To avoid the influence of signal crosstalk, the transmitted signal frequency of the second dissemination system was 9 GHz.

Because the reference signal of the 9 GHz dissemination system was 3.6 GHz. The 10 GHz received signal of remote 1 should be down-converted to 3.6 GHz as the microwave reference signal of the 9 GHz dissemination system through a low noise frequency conversion module. The schematic diagram of the low noise 10 GHz to 3.6 GHz frequency

conversion module is shown in Figure 4. A portion of the 10 GHz received signal from remote 1 was divided by 10 with a 10-prescaler, which generated a lot of harmonic components. We used two bandpass filters to select 4 GHz and 2 GHz harmonic signals. Then we divided the selected 2 GHz signal by 5. The resultant 400 MHz signal mixed with the selected 4 GHz signal. Thus, we were able to obtain a 3.6 GHz signal which was referenced to the 10 GHz received signal of the previous 10 GHz dissemination system.

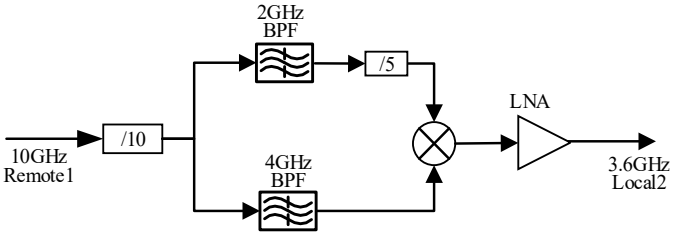

Figure 4. Scheme of the low-noise 10–3.6 GHz frequency conversion; LNA: low-noise amplifier; BPF: bandpass filter.

At remote 2, a 9 GHz PDRO referenced to 100 MHz OCXO was phase-locked to the 9 GHz received signal of remote 2. In this way, the output 100 MHz signal and 9 GHz signal can be synchronized to the H-maser at local 1 over the cascaded link simultaneously. During the signal light transferring along the fiber, a part of the signal light is reflected in the opposite direction due to Rayleigh scattering. If the local end site and the remote site use lasers with the same wavelength, the backscattered light interferes with the transmitted light field in the same direction, increasing the relative intensity noise of the PD output signal. Each dissemination system the wavelength optical difference carries between the local site and remote site was 0.8 nm, which can prevent the influence of coherent Rayleigh scattering.

Optical loss and dispersion of a fiber link deteriorates the signal-to-noise ratio of demodulated microwave signal; therefore, we also added a section of dispersion compensation fiber to compensate for the dispersion of the 106 km urban fiber link. Between the negative dispersion fiber and the urban fiber link, we used two bidirectional Erbium-doped fiber optical amplifiers (Bi-EDFA) to compensate for the additional 9 dB losses introduced by the negative dispersion fiber and the loss of urban link.

Before each photodiode, we used a unidirectional Erbium-doped fiber optical amplifiers (EDFA) working in automatic power control mode (APC), which kept the input optical power of each photodiode constant. Thus, the power of the microwave signal output from the photodiodes was constant, reducing amplitude-modulation-to-phase-modulation (AM/PM) conversion noise.

4. Results and Discussion

We obtained the dissemination stability over the cascaded link by analyzing the phase variation between the recovered 9 GHz signal of remote 2 and the 4 GHz reference signal of local 1 through converting the 9 GHz recovered signal to the 4 GHz signal. We also measured the stability of each segment of the cascaded system, which contained two microwave frequency dissemination systems and a low-noise 10 GHz to 3.6 GHz frequency-conversion module.

In general, the frequency stability was measured with commercial devices such as a frequency counter and the Phase Noise and Allan Deviation Test Set (for example Symmetricom Corporation 5125A). However, the measurement noise floor of the frequency counter cannot meet our requirements. The measurement range of the Phase Noise and Allan Deviation Test Set 5125A is below 400 MHz and only one 5125A was available. Consequently, we used a voltmeter to measure the stability of 9 GHz recovered signal at remote 2. The measurement scheme is shown in Figure 5.

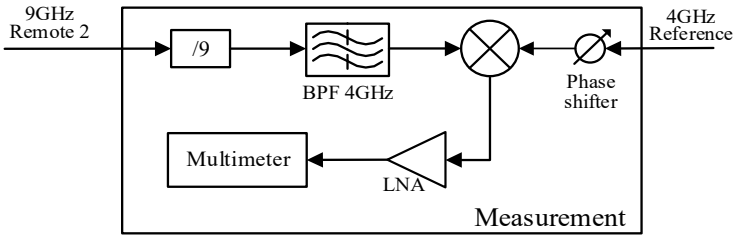

Figure 5. Stabilities measurement scheme; LNA: low-noise amplifier; BPF: band pass filter.

We converted the 9 GHz recovered signal into the 1 GHz signal using a 9-prescaler with many harmonic components. Then, we used a 4 GHz band pass filter to select 4 GHz signal (fourth harmonic wave). The phase fluctuation of the 4th harmonic wave is proportional to that of 9 GHz recovered signal. The 4 GHz reference signal of local 1 was down-converted to DC by mixing with the selected 4 GHz signal (fourth harmonic wave). The DC voltage corresponded to the relative phase delay fluctuation $x(t)$ between two 4 GHz signals with a relation of $V(t) = \frac{V_{pp}}{2} sin(2\pi f x(t))$. In this formula, the frequency of the mixed signal f is 4 GHz. V_{pp} is the peak-to-peak voltage of the DC signal when the phase of the 4 GHz reference signal changes more than 2π (controlled by the phase shifter). $x(t)$ is the real-time relative phase-delay fluctuation between two 4 GHz signals. $V(t)$ is the real-time voltage fluctuation of the DC signal as measured by a multimeter (Keysight 3458A) and recorded by a computer at one-second intervals. Next, we calculated a set of phase-delay values $x(t)$ according to the formula. Then we calculated the overlapping Allan deviation of $x(t)$. The stability of each microwave frequency dissemination system over the 106 km single-stage urban fiber link was measured with the same stability measurement technique.

To evaluate the characteristic of phase noise of this cascaded link, we measured the residual phase noise of the recovered 100 MHz signal of remote 2 using the Phase Noise Test Set 5125A; the results are shown in Figure 6 curve (a). For parallel cascaded stages, the phase noise accumulated along the fiber link is the same. In order to evaluate the link noise-suppression effect, we measured the free-running noise of the 106 km fiber link. According to the principle of the microwave frequency dissemination system, the pre-compensated phase of 100 MHz OCXO at the local site was equal to the noise of the fiber link, so we obtained the free-running fiber link noise by comparing the phase of the pre-compensated 100 MHz signal at local 2 with the phase of the recovered 100-MHz signal at remote 2, using the Phase Noise Test Set 5125A (see Figure 6 curve (b)). The bump around 10 Hz–40 Hz was the acoustic noise along the fiber link. Unlike the residual phase-noise of dissemination over fiber spools, this kind of acoustic noise only appears in urban fiber, which can be attributed to mechanical vibration along the fiber link. Peak 1 at about 300 Hz was caused by the bandwidth of the phase-locked loop of the 10 GHz dissemination system. Peak 2, at 384 Hz, was caused by the bandwidth of the phase-locked loop of the 9 GHz dissemination system.

Figure 7 shows the phase-delay fluctuation of dissemination over the 212 km cascaded link (2-stage) and 212 km single-stage link. In Figure 7, curve (a) shows the phase-delay fluctuation of the 9 GHz received signal at remote2 compared with the reference 4 GHz signal at Local 1. For comparison, we performed a microwave frequency dissemination experiment over the whole 212 km single-stage urban link, using the 10 GHz dissemination system. The phase-delay fluctuation of the 10 GHz signal over the 212 km single-stage link is shown in curve (b). The greater PLL correction bandwidth of the cascaded system was able to suppress more phase noise than the single-stage system (the bandwidth of single-stage system below 285 Hz). The delay fluctuation over the 212 km cascaded link was smaller than that over the 212 km single-stage link.

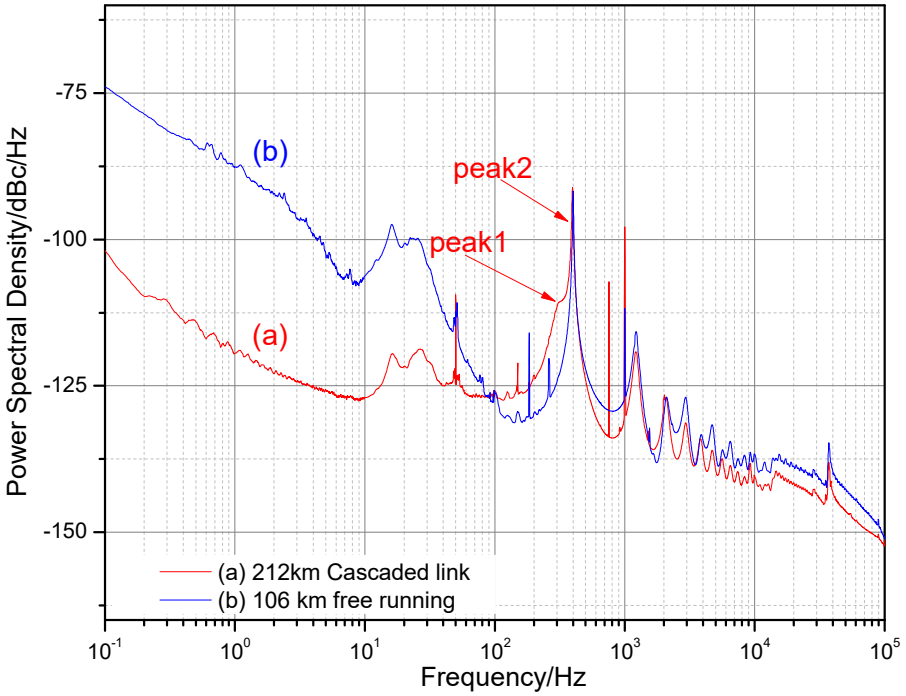

Figure 6. Residual phase noise of the cascaded system.

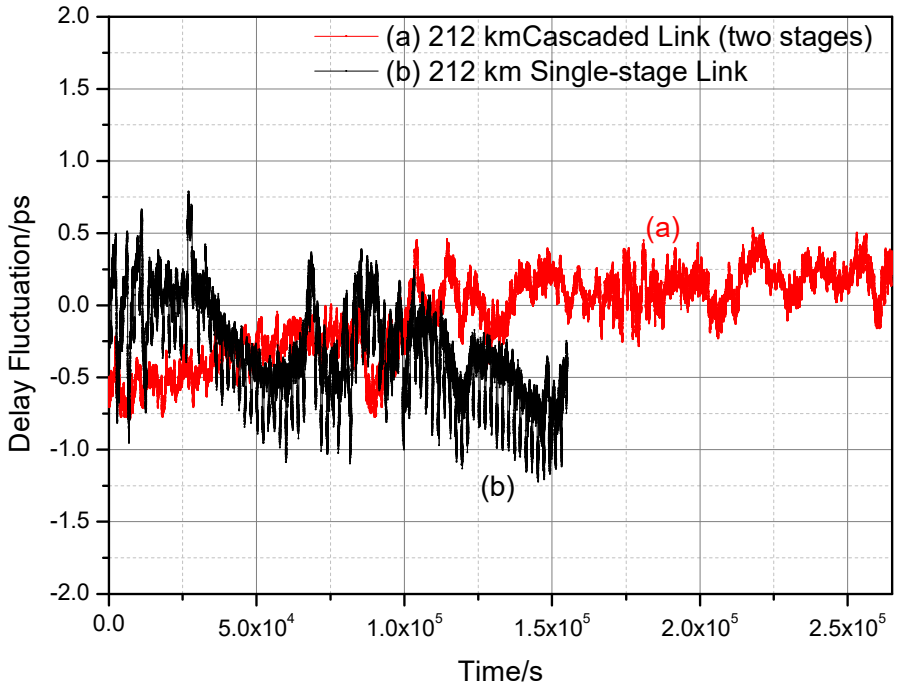

Figure 7. Delay fluctuation of the cascaded dissemination system.

In Figure 8, curve (a) shows the stability of the 10 GHz dissemination system, which was 3.06×10^{-15} at 1s and 2.34×10^{-17} at 10^4 s. Curve (b) shows the stability of the 9 GHz dissemination system, which was 3.03×10^{-15} at 1s and 1.39×10^{-17} at 10^4 s. Curve (c) shows the stability of the 10 GHz to 3.6 GHz low-noise frequency conversion (LN frequency conversion).

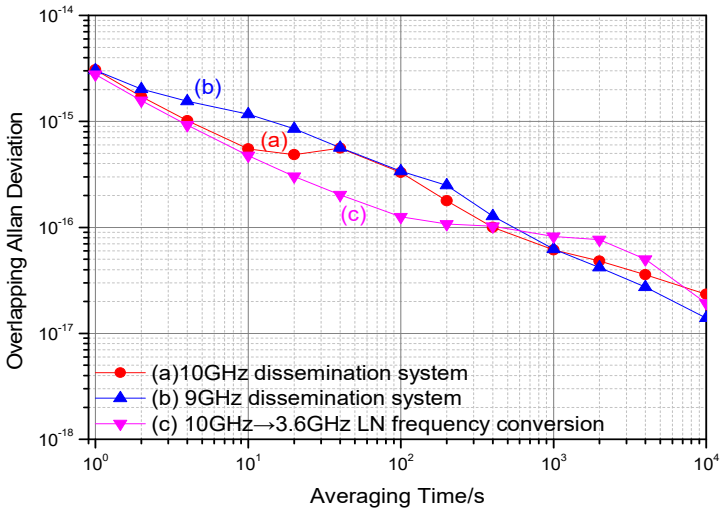

Figure 8. Stability of each segment.

In Figure 9, curve (a) shows the frequency dissemination stability over a 212 km cascaded urban link, which was 6.2×10^{-15} at 1s and 6.4×10^{-18} at 40,000 s. For the frequency dissemination over the cascaded link each segment can be considered as independent. The stability of the cascaded link can be expressed as the root-sum-square of each segment depicted in curve (b). For the stability of each stage, the stability is determined by the received signal relative to the reference signal of the same stage, which does not consider the accumulation of phase noise deterioration between segments. The calculated stability is better than that of measurement stability in 1000 s averaging time. Curve (c) shows the dissemination stability over the 212 km single-stage urban fiber: 1.6×10^{-14} at 1s and 2.7×10^{-16} at 1000 s. Benefiting from the greater correction bandwidth of the cascaded frequency dissemination system, the cascaded system was able to suppress more phase noise introduced by the fiber link than the single-stage system. The transfer stability of the 212 km cascaded link is better than that of the 212 km single-stage link. However, further improvement of the stability of the cascaded transfer system is mainly limited by the noise floor of the single-stage dissemination system.

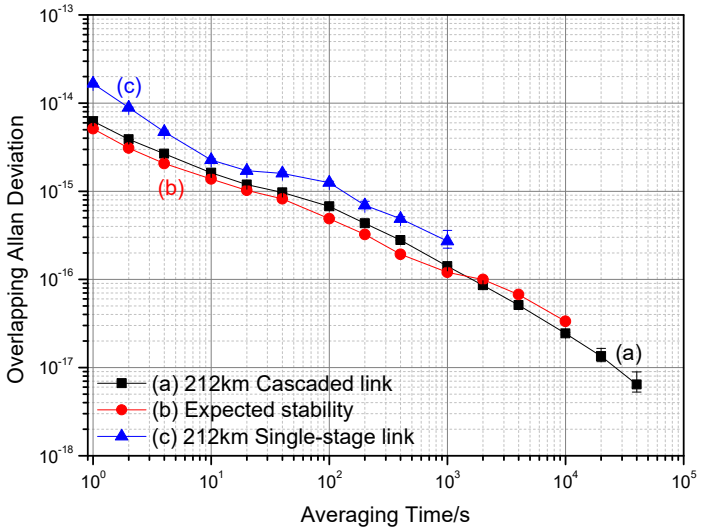

Figure 9. Dissemination stability of the 212 km urban link.

In this system, the asymmetry of the fiber link is derived from the group velocity dispersion (GVD). Based on the phase noise cancellation scheme, we assumed that the forward transmission signal and back transmission signal would go through the same fiber

link with the same delay τ; however, τ is closely related to the wavelength of the optical carrier and the temperature fluctuation [27]. The chromatic propagation delay uncertainty can be calculated as: $\Delta\tau = (\lambda_1 - \lambda_2)D(T)L$. The chromatic dispersion coefficient $D(T)$ (ps·nm^{-1}·km^{-1}) is related to outdoor temperature T. L is the entire length of the fiber link. In SM-28e fiber, $\frac{\partial D}{\partial T} = 1.45 fs/(nm \times km \times K)$. When the experiment was conducted the outdoor temperature fluctuated about 13 °C in one day. Though the urban fiber link we used was laid underground, the burial depth was not enough to insulate it from temperature changes completely. Therefore, the delay uncertainty was about 1.2 ps due to temperature fluctuations, which deteriorated the long-term transfer instability. If we can make the wavelength difference smaller, the long-term stability can be optimized.

5. Conclusions

We demonstrated a microwave frequency dissemination experiment over a 212 km cascaded urban link, which exhibited frequency stabilities of 6.2×10^{-15} at 1s and 6.4×10^{-18} at 40,000 s. Frequency dissemination over a cascaded link has a larger correction bandwidth compared with the bandwidth of single stage dissemination with the same distance. Benefiting from the large phase-noise suppression bandwidth of a cascaded urban link, the delay fluctuation of the cascaded link was smaller than that of a single-stage link with the same length. Furthermore, the dissemination stability of the 212 km cascaded link was better than that of 212 km single-stage link. In the next step of our research, we will investigate frequency dissemination over a longer distance through cascaded scheme.

Author Contributions: Conceptualization, H.Q., W.X. and W.Z.; Data curation, H.Q. and W.X.; Formal analysis, H.Q., W.Z. and H.J.; Funding acquisition, S.Z.; Methodology, H.Q., Y.X. and W.Z.; Software, W.X.; Supervision, S.Z., W.G. and H.J All authors have read and agreed to the published version of the manuscript.

Funding: The Western Light Project, Chinese Academy of Sciences (No. 29202082).

Conflicts of Interest: The authors declare no conflict of interest.

References

1. Calhoun, M.; Huang, S.; Tjoelker, R.L. Stable Photonic Links for Frequency and Time Transfer in the Deep-Space Network and Antenna Arrays. *Proc. IEEE* **2007**, *95*, 1931–1946. [CrossRef]
2. Gozzard, D.R.; Schediwy, S.W.; Dodson, R.; Rioja, M.J.; Hill, M.; Lennon, B.; McFee, J.; Mirtschin, P.; Stevens, J.; Grainge, K. Astronomical Verification of a Stabilized Frequency Reference Transfer System for the Square Kilometer Array. *Astron. J.* **2017**, *154*, 9. [CrossRef]
3. He, Y.; Baldwin, K.G.H.; Orr, B.J.; Bruce Warrington, R.; Wouters, M.J.; Luiten, A.N.; Mirtschin, P.; Tzioumis, T.; Phillips, C.; Stevens, J.; et al. Long-distance telecom-fiber transfer of a radio-frequency reference for radio astronomy. *Optica* **2018**, *5*, 138–146. [CrossRef]
4. Clivati, C.; Aiello, R.; Bianco, G.; Bortolotti, C.; De Natale, P.; Di Sarno, V.; Maddaloni, P.; Maccaferri, G.; Mura, A.; Negusini, M.; et al. Common-clock very long baseline interferometry using a coherent optical fiber link. *Optica* **2020**, *7*, 1031. [CrossRef]
5. Schioppo, M.; Kronjager, J.; Silva, A.; Ilieva, R.; Paterson, J.W.; Baynham, C.F.A.; Bowden, W.; Hill, I.R.; Hobson, R.; Vianello, A.; et al. Comparing ultrastable lasers at 7×10^{-17} fractional frequency instability through a 2220 km optical fibre network. *Nat. Commun.* **2022**, *13*, 212. [CrossRef]
6. Delva, P.; Lodewyck, J. Atomic clocks: New prospects in metrology and geodesy. *Acta Futur.* **2013**, *7*, 67–78. [CrossRef]
7. Wu, K.; Shen, Z.; Shen, W.; Sun, X.; Cai, C.; Wu, Y. A preliminary experiment of determining the geopotential difference using two hydrogen atomic clocks and TWSTFT technique. *Geod. Geodyn.* **2020**, *11*, 229–241. [CrossRef]
8. Uzan, J.-P. The fundamental constants and their variation: Observational status and theoretical motivations. *Physics* **2002**, *75*, 403–455. [CrossRef]
9. Czubaa, K.; Eintsb, F.; Felber, M.; Dobrowolski, J.; Simrock, S. First Generation of Optical Fiber Phase Reference Distribution System for TESLA. *Elektronika* **2005**. [CrossRef]
10. Hong, H.; Quan, R.; Xiang, X.; Xue, W.; Quan, H.; Zhao, W.; Liu, Y.; Cao, M.; Liu, T.; Zhang, S.; et al. Demonstration of 50 km Fiber-optic two-way quantum clock synchronization. *J. Lightwave Technol.* **2022**, *40*, 3723–3728. [CrossRef]
11. Bauch, A.; Achkar, J.; Bize, S.; Calonico, D.; Dach, R.; Hlavać, R.; Lorini, L.; Parker, T.; Petit, G.; Piester, D.; et al. Comparison between frequency standards in Europe and the USA at the 10−15 uncertainty level. *Metrologia* **2006**, *43*, 109–120. [CrossRef]

12. Kong, Y.; Yang, X.; Chang, H.; Qin, W.; Cao, F.; Li, Z.; Sun, B. Method of Precise Common-View frequency transfer based on BeiDou GEO satellite. In Proceedings of the 2014 IEEE International Frequency Control Symposium (FCS), Taipei, Taiwan, 19–22 May 2014; pp. 1–4.
13. Droste, S.; Grebing, C.; Leute, J.; Raupach, S.M.F.; Matveev, A.; Hänsch, T.W.; Bauch, A.; Holzwarth, R.; Grosche, G. Characterization of a 450 km baseline GPS carrier-phase link using an optical fiber link. *New J. Phys.* **2015**, *17*, 83044. [CrossRef]
14. Sun, S.C.; Bai, Y.; Liang, H.J.; Wang, S.G.; Wang, L.J. Ground-to-satellite time and frequency synchronization link with active carrier phase compensation. *Rev. Sci. Instrum.* **2019**, *90*, 114708. [CrossRef] [PubMed]
15. Newbury, N.R.; Williams, P.A.; Swann, W.C. Coherent transfer of an optical carrier over 251 km. *Opt. Lett.* **2007**, *32*, 3056–3058. [CrossRef] [PubMed]
16. Jiang, H.; Kefelian, F.; Crane, S.; Lopez, O.; Lours, M.; Millo, J.; Holleville, D.; Lemonde, P.; Chardonnet, C.; Amy-Klein, A.; et al. Long-distance frequency transfer over an urban fiber link using optical phase stabilization. *J. Opt. Soc. Am. B* **2008**, *25*, 2029–2035. [CrossRef]
17. Williams, P.A.; Swann, W.C.; Newbury, N.R. High-stability transfer of an optical frequency over long fiber-optic links. *J. Opt. Soc. Am. B* **2008**, *25*, 1284–1293. [CrossRef]
18. Fujieda, M.; Kumagai, M.; Gotoh, T.; Hosokawa, M. Ultrastable Frequency Dissemination via Optical Fiber at NICT. *IEEE Trans. Instrum. Meas.* **2009**, *58*, 1223–1228. [CrossRef]
19. Daussy, C.; Lopez, O.; Amy-Klein, A.; Goncharov, A.; Guinet, M.; Chardonnet, C.; Narbonneau, F.; Lours, M.; Chambon, D.; Bize, S.; et al. Long-distance frequency dissemination with a resolution of 10^{-17}. *Phys. Rev. Lett.* **2005**, *94*, 203904. [CrossRef] [PubMed]
20. Lopez, O.; Amy-Klein, A.; Lours, M.; Chardonnet, C.; Santarelli, G. High-resolution microwave frequency dissemination on an 86-km urban optical link. *Appl. Phys. B* **2009**, *98*, 723–727. [CrossRef]
21. Chunhao, H.; Zhiwu, C.; Yuting, L.; Li, L.; Shenghong, X.; Lingfeng, Z.; Xianglei, W. Time Synchronization and Performance of BeiDou Satellite Clocks in Orbit. *Int. J. Navig. Obs.* **2013**, *2013*, 1–5. [CrossRef]
22. Wang, B.; Gao, C.; Chen, W.L.; Miao, J.; Zhu, X.; Bai, Y.; Zhang, J.W.; Feng, Y.Y.; Li, T.C.; Wang, L.J. Precise and continuous time and frequency synchronisation at the 5×10^{-19} accuracy level. *Sci. Rep.* **2012**, *2*, 556. [CrossRef]
23. Liu, Q.; Chen, W.; Xu, D.; Cheng, N.; Yang, F.; Gui, Y.; Cai, H.; Han, S. Simultaneous Frequency Transfer and Time Synchronization over a Cascaded Fiber Link of 230 km. *Chin. J. Lasers* **2016**, *43*, 305006. [CrossRef]
24. Gao, C.; Wang, B.; Zhu, X.; Yuan, Y.B.; Wang, L.J. Dissemination stability and phase noise characteristics in a cascaded, fiber-based long-haul radio frequency dissemination network. *Rev. Sci. Instrum.* **2015**, *86*, 093111. [CrossRef] [PubMed]
25. US Department of Commerce, N. Handbook of Frequency Stability Analysis. *NIST SP-1065* **2007**, *1065*, 1–123.
26. Liao, R.; Lu, L.; Zhu, Y.; Wu, C.; Zhang, B.; Yu, L. Impact of Frequency Crosstalk on Fiber Frequency Transfer Performance. *Acta Opt. Sin.* **2017**, *37*, 7. [CrossRef]
27. Wang, B.; Zhu, X.; Gao, C.; Bai, Y.; Dong, J.W.; Wang, L.J. Square Kilometre Array Telescope–Precision Reference Frequency Synchronisation via 1f-2f Dissemination. *Sci. Rep.* **2015**, *5*, 13851. [CrossRef] [PubMed]